

Tensor polarizability of the ground-state hyperfine structure of thallium*

Harvey Gould[†]

Department of Physics, Brandeis University, Waltham, Massachusetts 02154

(Received 17 June 1974; revised manuscript received 15 March 1976)

The atomic-beam magnetic-resonance technique has been used to measure the hyperfine-structure tensor polarizability (quadratic Stark effect) in the $6^2P_{1/2}$ ground state of atomic thallium. Electric fields of up to 460 kV/cm were used to lift the degeneracy between the $m_F = 0$ and the $m_F = \pm 1$ substates in the absence of an external magnetic field, and focusing transitions between these Stark-separated states were observed. Measurements were also made between Zeeman-separated substates. The results are $\alpha_T = -(3.74 \pm 0.09) \times 10^{-8}$ Hz/(V/cm)², or $k = -(5.62 \pm 0.14) \times 10^{-8}$ Hz/(V/cm)², where $\delta\nu = kE^2$ is the Stark shift of the ($m_F = 0$) \leftrightarrow ($m_F = -1$) "flop-in" transition.

I. INTRODUCTION

This paper reports an atomic-beam magnetic-resonance measurement of the hyperfine-tensor polarizability in the $6^2P_{1/2}$ ground state of atomic thallium. The hyperfine-structure Stark effect in a state of electronic angular momentum J is related to the scalar and tensor polarizabilities by the formula¹

$$\Delta W = -\frac{\alpha_S(J)E^2}{2} - \frac{\alpha_T(J)}{4} \frac{3m_F^2 - F(F+1)}{F(2F-1)} (3E_z^2 - E^2), \quad (1)$$

where E_z is the "z" component of the electric field E , m_F is the Zeeman substate of F , the total (electronic plus nuclear) angular momentum, and α_S and α_T are the scalar and tensor hyperfine polarizabilities. The polarizability is defined¹ in terms of the $m_F = F$ stretched-state matrix element of the Stark operator, $T_S^{(2)}$,

$$-\frac{1}{4}\alpha_T(J, F)(3E_z^2 - E^2) = \langle J, F, m_F = F | T_S^{(2)} | J, F, m_F = F \rangle \quad (2)$$

so that in a uniform electric field in the z direction the polarizability of the stretched state is given by

$$\Delta W = -\frac{1}{2}\alpha_T(J, F)E^2. \quad (3)$$

Measurements of the Stark effect between different m_F^2 but the same F determine α_T . First-order Stark effects, linear in E and m_F , are prohibited by conservation of parity and time-reversal invariance, and have not been observed.²⁻⁵ [A linear Stark effect would arise from the interaction of the electric field with a permanent electric dipole moment (EDM) of the atom. The likely cause of any atomic EDM would be a permanent EDM of the electron.⁶] Measurement of the hyperfine-tensor polarizability in thallium is of particular interest because of

its connection with experiments to search for a permanent EDM of the electron.⁴ In particular, measurements between Stark-separated levels (see Sec. II) offer attractive possibilities for EDM measurements nearly free from instrumental effects caused by motional magnetic fields.²⁻⁴

At least two separate effects contribute to the hyperfine-tensor polarizability in the thallium ground state. First is a second-order perturbation involving the off-diagonal matrix element of the hyperfine-structure operator and the tensor Stark operator between P states.^{1,7,8} The contribution from the $6^2P_{3/2}$ state is given by

$$\Delta W = \frac{\langle P_{1/2} | O_{\text{hfs}} | P_{3/2} \rangle \langle P_{3/2} | T_S^{(2)} | P_{1/2} \rangle + \text{c.c.}}{W_{1/2} - W_{3/2}}. \quad (4)$$

Accurate evaluation of the off-diagonal matrix element is not straightforward owing to very large configuration-interaction effects.⁹ An approximate value can be obtained from Zeeman-effect measurements of Fowler.¹⁰ The most probable value is -1.1 GHz and the lower limit is -0.7 GHz. The off-diagonal matrix element of the tensor Stark operator can be evaluated in terms of the diagonal matrix element of the tensor Stark operator in the $6^2P_{3/2}$ state and hence the tensor polarizability in that state. We find

$$\langle P_{3/2} | T_S^{(2)} | P_{1/2} \rangle = \sqrt{2} \langle P_{3/2} | T_S^{(2)} | P_{3/2} \rangle \quad (5)$$

The tensor polarizability in the metastable $6^2P_{3/2}$ state has been measured by Petersen *et al.*¹¹ They find $\alpha_T(\frac{3}{2}) = (-6.02 \pm 0.08) \times 10^{-3}$. Using $W_{3/2} - W_{1/2} = 7793 \text{ cm}^{-1}$,¹² the contribution to $\alpha_T(\frac{1}{2})$ is $-8 \times 10^{-8} \text{ Hz/(V/cm)}^2$. The contribution to the ground-state hyperfine-tensor polarizability from the $6^2P_{3/2}$ state is not the only, nor necessarily the largest contribution. The $7^2P_{3/2}$ and $8^2P_{3/2}$ states lie 35 000 and 42 000 cm^{-1} above the ground state and the series limit is at 49 000 cm^{-1} . Contri-

butions from the ${}^2P_{1/2}$ states will also be present. These states, compared to the $6^2P_{3/2}$ state, do not lie far enough above the ground state (as in the case of the $3^2P_{3/2}$ state in aluminum) to neglect their effect upon $\alpha_T(\frac{1}{2})$. The polarizabilities of these states are not yet known, without which their contribution to $\alpha_T(\frac{3}{2})$ can not be estimated.

The second effect is a third-order effect involving the hyperfine structure in excited states.^{1,13} This is the same interaction which gives rise to the ground-state hyperfine-tensor polarizabilities in the alkali atoms. If one neglects all but the $7^2S_{1/2}$ state, the interaction takes the form¹³

$$\Delta W = \frac{\langle P_{1/2} | z | S_{1/2} \rangle \langle S_{1/2} | O_{\text{hfs}} | S_{1/2} \rangle \langle S_{1/2} | z | P_{1/2} \rangle}{(W_{6P} - W_{7S})^2} eE^2. \quad (6)$$

The quantity $|\langle P_{1/2} | z | S_{1/2} \rangle|^2 / (W_{6P} - W_{7S})$ is of the form of the (atomic) scalar polarizability, and evaluation by a Bates-Damgaard calculation¹⁴ gives $2.4 \times 10^{-24} \text{ cm}^3$. Using the experimental value¹⁵ of 0.417 cm^{-1} for the $7^2S_{1/2}$ hyperfine-structure splitting, and $W_{7S} - W_{6P} = 26478 \text{ cm}^{-1}$,¹² the contribution to $\alpha_T(\frac{1}{2})$ is $-1.6 \times 10^{-8} \text{ Hz}/(\text{V}/\text{cm})^2$.

Both of the interactions result in an electric

TABLE I. Hyperfine-structure tensor polarizabilities.

Element	State	$\alpha_T(\text{expt})$ [Hz/(V/cm) ²]	$\alpha_T(\text{calc})$ [Hz/(V/cm) ²]
Cs	$6^2S_{1/2}$	$-3.66 \times 10^{-8} \text{ a}$	$-4.13 \times 10^{-8} \text{ b}$
^{87}Rb	$5^2S_{1/2}$	$-1.39 \times 10^{-8} \text{ a}$	$-2.00 \times 10^{-8} \text{ b}$
^{85}Rb	$5^2S_{1/2}$	$-4.56 \times 10^{-9} \text{ a}$	$-7.8 \times 10^{-9} \text{ b}$
K	$4^2S_{1/2}$	$-6.4 \times 10^{-10} \text{ a}$	$-9.3 \times 10^{-10} \text{ b}$
Na	$3^2S_{1/2}$	$-1.5 \times 10^{-9} \text{ a}$	$-1.7 \times 10^{-9} \text{ b}$
Li	$2^2S_{1/2}$	$+3.0 \times 10^{-10} \text{ b}$	$-7 \times 10^{-10} \text{ b}$
Al	$3^2P_{3/2}$	$-2.0 \times 10^{-3} \text{ c}$	
Al	$3^2P_{1/2}$	$+2.0 \times 10^{-7} \text{ c, d}$	$+2.0 \times 10^{-7} \text{ c, d}$
Tl	$6^2P_{1/2}$	$-3.74 \times 10^{-8} \text{ e}$	See text
Tl	$6^2P_{3/2}$	$-6.04 \times 10^{-3} \text{ f}$	
Sm	$4f^6 6s^2 {}^7F_6$	$-9.1 \times 10^{-4} \text{ c}$	See Ref. 8
Eu	$4f^7 6s^2 {}^8S_{7/2}$	$+3.51 \times 10^{-6} \text{ c}$	

^a Reference 16.

^b Reference 17.

^c References 7 and 8.

^d The only significant contribution to $\alpha_T(\frac{1}{2})$ is from the $P_{3/2}$ state [Eq. (2)] because of the small fine structure (112 cm^{-1}) in aluminum.

^e For preliminary results from an earlier attempt to measure $\alpha_T(\frac{1}{2})$ see T. S. Stein, J. P. Carrico, and E. Lipworth, Proceedings of DEAP., Physics of Free Atoms Conference, Berkeley, Calif. 1966, p. 12 (unpublished).

^f Reference 11.

field raising the energy of the $m_F = \pm 1$ levels and decreasing the energy of the $m_F = 0$ state. The signs and the magnitude of these effects are in general agreement with the experiment.

The hyperfine-tensor polarizabilities have been measured in the alkali metals, some of the group-III A elements, and a few of the rare earths. Values are listed in Table I.

II. METHOD

Details of the standard techniques of Stark-effect measurement by atomic-beam magnetic resonance may be obtained from Refs. 8, 13, 16, and 17.

As Table I shows, some of the hyperfine-tensor polarizabilities measured to date are very small. As a result, a standard feature of these experiments has been the use of a magnetic field to remove the degeneracy between the m_F sublevels of the hyperfine structure. With the sublevels separated by the Zeeman effect, the resonance frequency of the $\Delta F = 0$, $(m_F = -F) \leftrightarrow (m_F = -F + 1)$ refocusing transition is monitored as a function of the applied electric field parallel to the magnetic field. Stark shifts which are small compared to the several hundred Hz resonance linewidths (obtained from a 1-m interaction region) are measured using slope detection.^{13,16,17}

Thallium possesses a large ground-state hyperfine splitting⁹⁻¹¹ (Fig. 1) which prevents the complete decoupling of the nuclear and electronic angular momentum by the inhomogeneous magnetic field used to deflect the atoms in the atomic-beam resonance apparatus. Atoms in states of the same m_J but different m_F suffer different deflections in

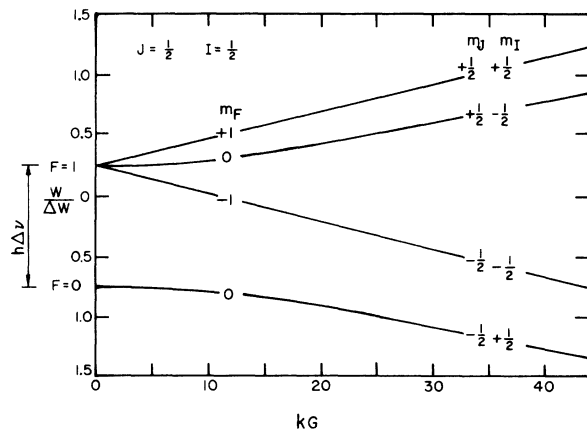


FIG. 1. Breit Rabi diagram for $6^2P_{1/2}$ ground state of thallium. The hyperfine-structure separation $\Delta\nu$ is 21 GHz, g_J is $\frac{2}{3}$. The magnetic field in the deflecting magnets was between 11 and 24 kG depending upon the location of the atoms between the pole tips.

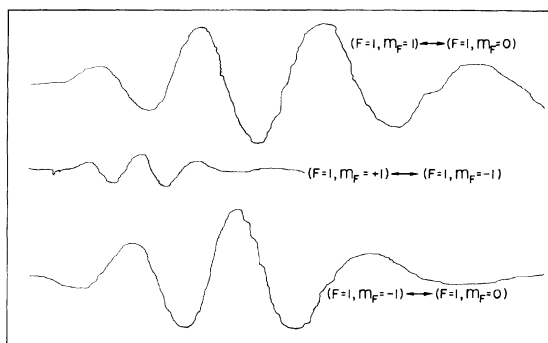


FIG. 2. Observed Ramsey patterns of the transitions between the three Zeeman sublevels of the $F=1$ state. The magnetic field is about 1 G and the electric field was 240 kV/cm. The resonance height of the single quantum transitions is 2×10^{-10} A.

the inhomogeneous magnets, and focusing transitions between these states can be observed in a carefully aligned apparatus. All three $\Delta F=0$ carelessly between the substates $m_F=1$, $m_F=0$, and $m_F=-1$ were observed (Fig. 2), as were the Stark effects (Fig. 3) in the $\Delta F=0$, ($m_F=1$) \leftrightarrow ($m_F=0$) and the $\Delta F=0$, ($m_F=-1$) \leftrightarrow ($m_F=0$) transitions. The multiple quantum transition ($m_F=1$) \leftrightarrow ($m_F=-1$) does not exhibit a Stark effect.

In a strong electric field it is possible to lift the degeneracy between the states of different m_F^2 in the absence of an external magnetic field¹³ (Fig. 4-6). If the m_J or m_F substates have been spatially separated by the first deflecting magnet

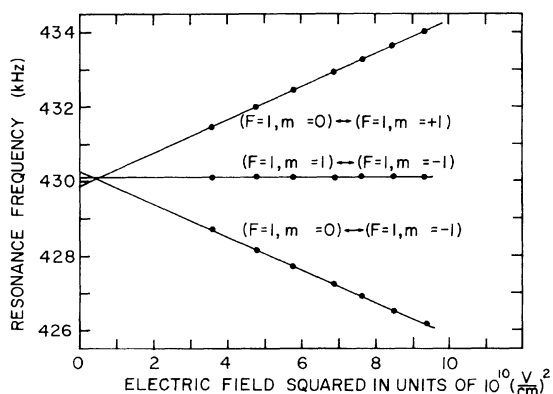


FIG. 3. Observed Stark effects in the transitions between the Zeeman sublevels of the $F=1$ state. The three transitions required different rf power levels, with the ($m_F=0$) \leftrightarrow ($m_F=1$) requiring the most power and the ($m_F=0$) \leftrightarrow ($m_F=-1$) requiring the least. Power shifts may have resulted in the nonzero intercepts. The rf power for a given transition was held constant for all the electric field values. No rf power dependence upon the quadratic Stark effect was observed. See Ref. 16.

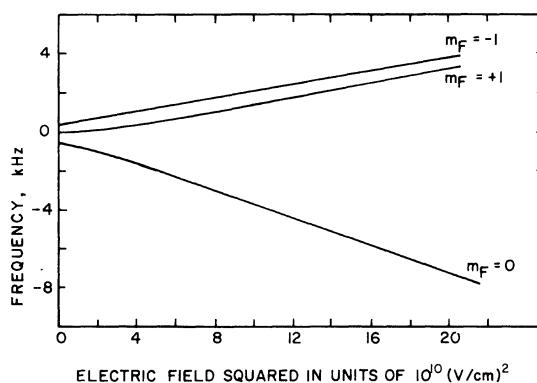


FIG. 4. Thallium $F=1$ energy levels for combined Stark and Zeeman effects. The energy levels represent those of a typical experiment in which there are residual magnetic fields of 0.7 mG (see Fig. 6) both parallel and perpendicular to the electric field, as well as the motional magnetic field experienced by an atom moving at 3×10^4 cm/sec. There is a slight departure from E^2 dependence for electric fields below 200 kV/cm.

(magnet A of Fig. 7), then transitions induced by an rf field between the Stark-separated $m_F=+1$ and $m_F=0$ states will be partially refocused by the second deflecting magnet (magnet B). In first order, the transition energy is given by formula (1).

As it is not possible to position the electrically conducting rf loops between the electrodes, they are placed in front and behind them. If end effects from the electric-field plates were neglected, the rf loops would be in a region of zero dc electric and magnetic fields. Inducing transitions with rf loops situated in zero external field is just a special case of a Ramsey double-loop resonance in which the interaction energy between the loops dif-

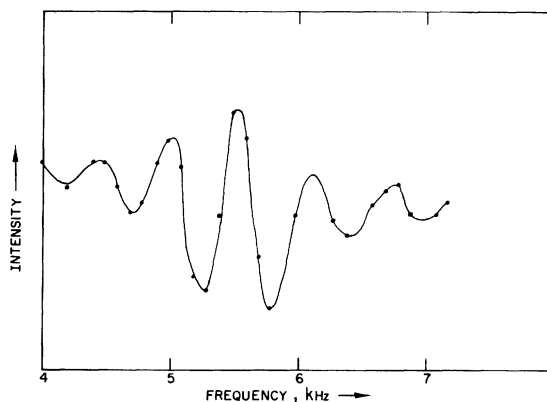


FIG. 5. Observed Ramsey pattern of the transition between the Stark-separated levels ($F=1$, $m_F=1$) \leftrightarrow ($F=1$, $m_F=0$) at an electric field of 365 kV/cm. The amplitude of the central peak is 3×10^{-11} A on top of the background of almost 10^{-9} A.

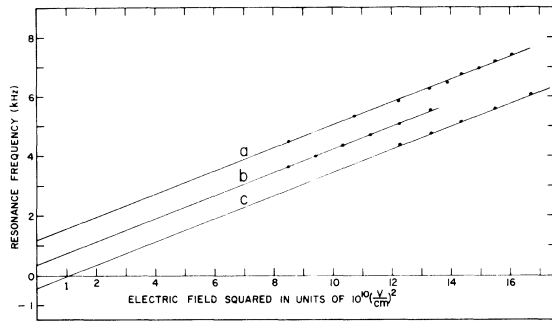


FIG. 6. Observed frequency of the $(m_F = \pm 1) \leftrightarrow (m_F = 0)$ transition between Stark-separated levels vs the electric field squared. The three runs are displaced from each other owing to different residual magnetic field in the interaction region. The residual magnetic fields resulted from saturation of a region of the hypernom shields by fringing fields from the deflecting magnets.

fers from the interaction energy at the loops.^{18, 19} A problem which arises from the lack of dc fields at the rf loops is that the m_F sublevels become degenerate, and the sublevels are mixed independent of the rf field. The focusing properties of the atoms becomes independent of the presence of the rf, and a resonance is no longer observed.²⁰ Failure to provide an external field at the rf loops greatly diminished resonance intensity for tensor-polarizability measurements made between Stark-separated levels (Fig. 5).

In the apparatus, the moving atoms will always be exposed to weak magnetic fields in the interaction region. An atom moving through an electric field \vec{E} experiences a motional magnetic field \vec{H} of $\vec{H} = (\vec{v}/c) \times \vec{E}$ which is perpendicular to both the electric field \vec{E} and the direction of motion of the atom. Typical values of $v \approx 3 \times 10^4$ cm/sec and $E = 3 \times 10^5$ V/cm = 1000 esu result in a motional magnetic field of 1 mG. The problem of combined

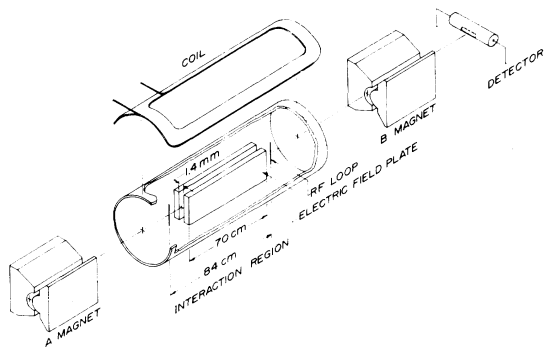


FIG. 7. Schematic diagram of atomic-beam magnetic-resonance apparatus. Only one of four magnetic field coils is shown.

Stark and Zeeman effects has been treated by several authors.²¹ Since the Stark and Zeeman effects of interest here are much smaller than the hyperfine-structure separation, only the three $F = 1$ levels need to be considered. Calculations of these effects in thallium show that, for a wide range of electric fields including those used in this tensor-polarizability measurement, deviations from quadratic behavior of the Stark effect are insignificant²² (Fig. 4).

III. APPARATUS

Thallium beams were produced from a resistively heated stainless-steel oven,²³ and detected by surface ionization on an (potassium) impurity-free oxidized-tungsten ribbon. The techniques used to make the impurity-free oxidized filament are described in the literature.^{10, 23, 24} The detector noise level was less than 10^{-13} A.

The interaction region (Fig. 7) contained glass electric-field plates, rf loops, and vertical and horizontal magnetic-field coils. The entire region was surrounded by three nested hypernom magnetic shields with end caps.

The electric-field plates (Fig. 8) made from common soda-lime glass sustained fields up to 450 kV/cm. The glass was made electrically conducting by heating to temperatures above 120°C . A detailed description of the present field plate assembly will be published elsewhere. Sim-

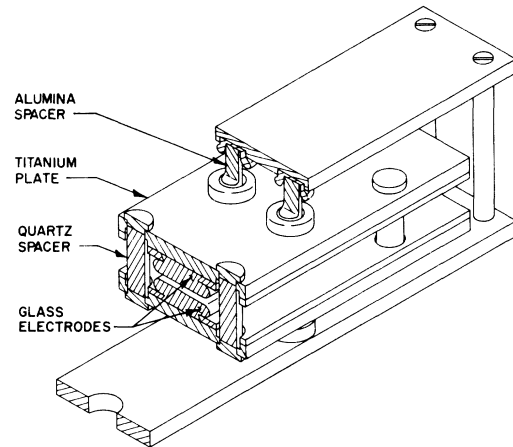


FIG. 8. Electric field plates. Two 70-cm-long glass electrodes with dovetail backs are clamped against titanium plates which in turn are held apart by quartz spacers. The titanium plates are held together by a second layer of plates. The second layer of plates, which are at ground potential, are heated by circulating hot glycerine through them. Heat is slowly transferred to the titanium plates and the glass electrodes by conduction through alumina spacers. When mounted in the apparatus, the gap is vertical.

pler systems utilizing a single glass plate (cathode) are described in Ref. 25.

IV. RESULTS

Results of tensor-polarizability measurements in the $F=1$ hyperfine state of the $^2P_{1/2}$ ground state of thallium are shown in Fig. 3 and Fig. 6, and in Table II. Three corrections have been applied to the data: first, a correction for the shift of the central peak of the Ramsey pattern which arises because the interaction energy at the rf loops is different from the average interaction energy between the loops^{18,19}; second, a filling factor correction which arises because atoms are subject to the electric field for only part of the time they are between the rf loops. These two effects require a combined correction of $\Delta\nu = \Delta\nu_0(1 + l/L) \times (L/d)$ where $\Delta\nu_0$ is the observed Stark shift, l is the width of the rf loops (1 cm), L is the separation between the rf loops (84 cm), and d is the length of the electric-field plates (70 cm). The third correction comes from a 3% decrease in the electric field caused by the loading of a resistor dividing chain.

The systematic effects associated with Stark-effect measurements between Zeeman-separated levels are well understood.^{8,13,16,17} The Stark-effect measurements performed on the Zeeman-separated states of the $F=1$ levels in thallium are relatively immune from all of the known effects. On the other hand, the measurements made between the Stark-separated levels are not. In particular, we consider the Bloch-Siegert effect.²⁶ If two oscillatory fields of different frequencies are present in the interaction region, then the central peak of the Ramsey pattern will be shifted by an amount^{19,27}

$$\delta\nu = (2b/2\pi)^2/2(\nu - \nu_1), \quad (7)$$

TABLE II. Results of tensor-polarizability measurements.

Between Zeeman-separated levels [10^{-8} Hz/(V/cm) ²]			
($F=1, m_F=1$)	($F=1, m_F=0$) flop out		-3.76 ± 0.03
($F=1, m_F=-1$)	($F=1, m_F=0$) flop in		-3.73 ± 0.02
Between Stark-separated levels [10^{-8} Hz/(V/cm) ²]			
Lowest frequency included	Graph a	Graph b	Graph c
All	-3.38	-3.40	-3.31
5 kHz	-3.48	-3.65	-3.56
6 kHz	-3.64		

TABLE III. Errors in Stark-effect measurement between Zeeman-separated levels.

Mechanical deflection of electric field plates due to electric field	$\leq 0.2\%$
Drift in electric and magnetic fields	$\leq 0.2\%$
Statistics	1.0%
Uncertainty in the filling factor	0.5%
Uncertainty in the electrode gap	1.0%
Uncertainty in the voltage measurement	<u>2.0%</u>
	2.5%

where $2b$ is the amplitude of the second oscillatory field of frequency ν_1 , and ν is the unshifted resonance frequency. Since oscillatory rather than rotating fields are used to induce the resonance, there will be an oppositely rotating component of the frequency corresponding to $-\nu$. Since this effect is largest at low frequencies, the net result is to decrease the slope of the observed frequency vs the electric-field-squared curve, resulting in a lower observed tensor polarizability. Estimates of $2b$ obtained from the criteria of maximum transition probability,²⁷ $2b(l/\alpha) = 0.6\pi$ (where α is the most probable velocity of an atom in the beam) result in shifts which are larger than the 10% discrepancy between the two techniques. Exact correction cannot be made without a detailed map of the beam profile and the distribution of rf amplitude within the loops as a function of both frequency and power level. From Eq. (7), however, it is expected that the effect would be smallest among points obtained at the highest transition frequencies. If measurements below 5 kHz are excluded (see Fig. 6 and Table II), the measured tensor polarizabilities rise to within 5% of the value obtained from measurements on Zeeman-separated levels. Excluding data below 6 kHz (curve c), the discrepancy is eliminated entirely.

Uncertainties in auxiliary measurements are the largest source of error in the Stark-effect measurements on the Zeeman-separated levels. The largest of these are the uncertainties in the voltage measurement and in the electric-field plate separation. A detailed list is given in Table III. The final result for the tensor polarizability of the $6^2P_{1/2}$ ground state of thallium is $\alpha_T = -(3.74 \pm 0.09) \times 10^{-8}$. This result is based upon the measurements between Zeeman-separated levels.

ACKNOWLEDGMENTS

The several hundred parts comprising the interaction region were masterfully constructed by the Brandeis University machine shop under the direction of Arthur Larsen. I thank Alan Ramsey

for continual help and advice; David Lillenfield and Yon Lee for their assistance; Professor Ezra Lipworth for support, encouragement and the stimulation which was instrumental in the comple-

tion of the work. I thank the University of California and the Lawrence Berkeley Laboratory for their hospitality during the final preparation of the manuscript.

*Work supported by the National Science Foundation.

†Present address: University of California, Lawrence Berkeley Lab., Berkeley, Calif. 94720.

¹J. R. P. Angel and P. G. H. Sandars, Proc. R. Soc. Lond. A 305, 125 (1968).

²M. C. Weisskopf, J. P. Carrico, H. Gould, E. Lipworth, and T. S. Stein, Phys. Rev. Lett. 21, 1645 (1968).

³M. A. Player and P. G. H. Sandars, J. Phys. B 3, 1620 (1970).

⁴H. Gould, Phys. Rev. Lett. 24, 1091 (1970).

⁵G. E. Harrison, P. G. H. Sandars, and J. J. Wright, Phys. Rev. Lett. 22, 1263 (1969); W. B. Dress *et al.*, Phys. Rev. 170, 1200 (1968); 179, 1285 (1969); V. W. Cohen *et al.*, Phys. Rev. 177, 1942 (1969).

⁶E. E. Salpeter, Phys. Rev. 112, 1642 (1958); M. Sachs, Phys. Lett. 14, 302 (1965); Ann. Phys. (N.Y.) 6, 224 (1959); L. I. Schiff, Phys. Rev. 132, 2194 (1963); P. G. H. Sandars, Phys. Lett. 14, 194 (1965); Phys. Lett. 22, 290 (1966); J. Phys. B 1, 499 (1968); 1, 511 (1968); V. K. Ignatovich, Zh. Eksp. Teor. Fiz. 56, 2019 (1969) [Sov. Phys.-JETP 29, 1084 (1969)]; R. M. Sternheimer, Phys. Rev. 183, 122 (1969); P. G. H. Sandars and R. M. Sternheimer, Phys. Rev. A 11, 473 (1975); Bull. Am. Phys. Soc. 20, 679 (1975).

⁷J. R. P. Angel, P. G. H. Sandars, and G. K. Woodgate, Proc. R. Soc. Lond. A 338, 95 (1974).

⁸N. J. Martin, P. G. H. Sandars, and G. K. Woodgate, Proc. R. Soc. Lond. A 305, 139 (1968).

⁹C. Schwartz, Phys. Rev. 97, 380 (1955); 105, 173 (1957); G. Gould, Phys. Rev. 101, 1828 (1956).

¹⁰T. K. Fowler, Ph.D. thesis (University of California, Berkeley, 1968) (unpublished report No. UCRL 18331).

¹¹F. R. Petersen, H. G. Palmer, and J. H. Shirley, Bull. Am. Phys. Soc. 13, 1674 (1968).

¹²C. E. Moore, *Atomic Energy Levels*, NBS Circ. No. 467 (U.S. GPO, Washington, D.C., 1958), Vol. III.

¹³E. Lipworth and P. G. H. Sandars, Phys. Rev. Lett. 13, 716 (1964).

¹⁴D. R. Bates and A. Damgaard, Phil. Trans. R. Soc. Lond. A 242, 101 (1949).

¹⁵S. Pollack and E. Wong, Am. J. Phys. 39, 1388 (1971).

¹⁶H. Gould, E. Lipworth, and M. C. Weisskopf, Phys. Rev. 188, 24 (1969), and references cited therein.

¹⁷J. P. Carrico *et al.*, Phys. Rev. 170, 64 (1968).

¹⁸N. F. Ramsey, Phys. Rev. 100, 1191 (1955).

¹⁹N. F. Ramsey, *Molecular Beams* (Oxford University, London, 1956), Chap. V, p. 143.

²⁰Reference 19, pp. 115 and 401.

²¹J. Yellin, Phys. Lett. 32A, 337 (1970); University of California Report No. UCRL 19569, 1970 (unpublished); J. R. Mowat (Brandeis University, 1972) (unpublished).

²²H. Gould (unpublished).

²³H. Gould, Ph.D. thesis (Brandeis University, 1970) Chap. III (available from University Microfilms, Ann Arbor, No. 70-24, 633, 1970).

²⁴E. F. Green, Rev. Sci. Instrum. 32, 860 (1961); E. E. Beehler and D. J. Glaze, IEEE Trans. Instrum. Meas. 15 (66).

²⁵R. Marrus, E. Wang, and J. Yellin, Phys. Rev. 177, 122 (1969). J. J. Murray, University of California Report No. UCRL 9506, 1960 (unpublished). Electric-field plates utilizing glass cathodes are in common use as beam separators for high-energy particle accelerators.

²⁶F. Bloch and A. Siegert, Phys. Rev. 57, 522 (1940).

²⁷Reference 19, Chap. V.